

Lipase-Sensitive Polymeric Triple-Layered Nanogel for “On-Demand” Drug Delivery

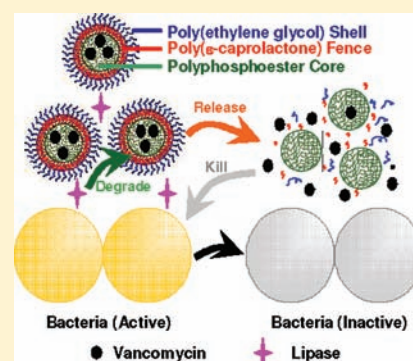
Meng-Hua Xiong,^{†,‡} Yan Bao,^{§,‡} Xian-Zhu Yang,[§] Yu-Cai Wang,[§] Baolin Sun,^{*,§} and Jun Wang^{*,§}

[†]CAS Key Laboratory of Soft Matter Chemistry and Department of Polymer Science and Engineering, University of Science and Technology of China, Hefei, Anhui 230026, China

[§]School of Life Sciences and Hefei National Laboratory of Physical Science at the Microscale, University of Science and Technology of China, Hefei, Anhui 230027, China.

Supporting Information

ABSTRACT: We report a new strategy for differential delivery of antimicrobials to bacterial infection sites with a lipase-sensitive polymeric triple-layered nanogel (TLN) as the drug carrier. The TLN was synthesized by a convenient arm-first procedure using an amphiphilic diblock copolymer, namely, monomethoxy poly(ethylene glycol)-*b*-poly(ϵ -caprolactone), to initiate the ring-opening polymerization of the difunctional monomer 3-oxapentane-1,5-diyl bis(ethylene phosphate). The hydrophobic poly(ϵ -caprolactone) (PCL) segments collapsed and surrounded the polyphosphoester core, forming a hydrophobic and compact molecular fence in aqueous solution which prevented antibiotic release from the polyphosphoester core prior to reaching bacterial infection sites. However, once the TLN sensed the lipase-secreting bacteria, the PCL fence of the TLN degraded to release the antibiotic. Using *Staphylococcus aureus* (*S. aureus*) as the model bacterium and vancomycin as the model antimicrobial, we demonstrated that the TLN released almost all the encapsulated vancomycin within 24 h only in the presence of *S. aureus*, significantly inhibiting *S. aureus* growth. The TLN further delivered the drug into bacteria-infected cells and efficiently released the drug to kill intracellular bacteria. This technique can be generalized to selectively deliver a variety of antibiotics for the treatment of various infections caused by lipase-secreting bacteria and thus provides a new, safe, effective, and universal approach for the treatment of extracellular and intracellular bacterial infections.



INTRODUCTION

Differential delivery of therapeutic agents to lesion sites is a central goal and key challenge in nanomedicine development.^{1,2} Nanoparticles can encapsulate drug molecules and may respond to the unique microenvironment of the targeted site, thus enabling the on-demand release of their cargo which achieves an ambitious goal of eliminating premature drug release at undesired sites.^{3,4} A responsive nanoparticulate drug delivery system can be activated by a range of stimuli such as pH,^{5–8} redox conditions,^{9–12} temperature,^{13,14} enzyme activity,^{15–18} competitive binding,^{19–21} magnetic actuation^{22–24} and photo-irradiation.^{25–28} Nanoparticles can be made from mesoporous silica,⁴ magnetic materials,^{29,30} interlayer cross-linked micelles,³¹ and other materials.^{32,33} Nevertheless, most of these materials are responsive to the unique, tumoral extracellular or intracellular environment, thereby exhibiting passive and active targeting effects in cancer therapy.

Bacterial infections cause significant amounts of fatalities and morbidities worldwide despite the availability of antibiotics.^{34,35} In addition, drug resistant strains of bacteria limit the choice of antibiotics, which has become a matter of worldwide concern.³⁶ Bacteria can also survive within cells (e.g., macrophages), evading the immune system, and thus protect themselves against the bactericidal action of antibiotics, leading to infection

recurrence.^{37,38} Recently, many efforts have been made to develop new materials for antibacterial drug discovery.^{39–41} As one of the most promising approaches, liposomes, polymeric nanoparticles, nanosuspensions, or conjugates, which can enhance the antibacterial activity and pharmacokinetic properties of antibiotics,^{42,43} can deliver these antibiotics. However, very few nanoparticulate delivery systems can respond to bacteria to achieve the on-demand release of antibiotics. Zhang and co-workers have reported the first example of this delivery method that responds to bacterially secreted toxins.³² This group developed chitosan-modified gold nanoparticles attached to the surface of liposomes which effectively prevent undesirable payload release in regular storage or physiological environments. However, once these protected liposomes “sense” bacteria that secrete toxins, encapsulated therapeutic agents are released and the bacteria are killed.

Herein, we report an entirely new strategy of differential delivery of antibiotics to treat bacterial infections, utilizing a bacterial-lipase sensitive polymeric triple-layered nanogel (TLN) as the nanocarrier. In this approach, the TLN contains a bacterial lipase-sensitive poly(ϵ -caprolactone) (PCL) inter-

Received: December 1, 2011

Published: February 3, 2012

layer between the cross-linked polyphosphoester core and the shell of poly(ethylene glycol) (Figure 1). Prior to reaching sites

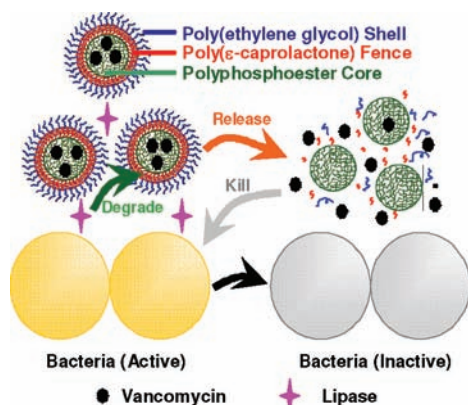


Figure 1. Schematic illustration of the on-demand drug delivery triggered by bacterial lipase to treat the bacterial infections using a polymeric triple-layered nanogel (TLN), which contains a bacterial lipase-sensitive poly(ϵ -caprolactone) (PCL) interlayer between the cross-linked polyphosphoester core and the shell of the poly(ethylene glycol).

of bacterial infection, the antibiotics are protected inside the polyphosphoester core and are not released due to the compacted PCL molecular fence surrounding the drug reservoir, eliminating potential adverse side effects due to premature drug leakage or nonspecific drug release. However, the PCL fence of TLN is subject to degradation by the activity of bacterial lipases, which are abundant in microbial flora since these enzymes are involved in bacterial lipid metabolism.^{44,45} A number of the pathogenic bacterial species have been proven to produce lipase which has been studied with respect to its role as a virulence factor in an infected human.⁴⁵ Therefore, this delivery method can lead to activated drug release and subsequently enhanced inhibition of bacteria growth.

EXPERIMENTAL SECTION

Materials. Dimethyl sulfoxide (DMSO) was dried over calcium hydride overnight and distilled under reduced pressure before use. Stannous octoate ($\text{Sn}(\text{Oct})_2$, Sinopharm Chemical Reagent Co., Ltd., China) was purified according to a method described in the literature.⁴⁶ Milli-Q water (18 M Ω) was prepared using a Milli-Q Synthesis System (Millipore, Bedford, MA, USA). The Agar A and lysostaphin were obtained from Sangon Biotech (Shanghai) Co., Ltd. (China). Lipase from *Pseudomonas cepacia* and alkaline phosphatase (ALP) were obtained from Sigma-Aldrich Chemical Co. Sepharose CL-4B was obtained from GE Healthcare. Bacto Tryptic Soy Broth (TSB) was obtained from BD Company. Vancomycin was obtained from Bio Basic Inc. Other reagents and solvents were used as described in the Supporting Information.

Synthesis of the Triple-Layered Nanogel (TLN). The syntheses of 3-oxapentane-1,5-diyl bis(ethylene phosphate) (DEGDP) and macroinitiator monomethoxy poly(ethylene glycol)-*b*-poly(ϵ -caprolactone) (mPEG-PCL) were described in the Supporting Information. mPEG-PCL (1.000 g, 0.093 mmol), DEGDP (0.088 g, 0.270 mmol), and DMSO (3.74 mL) were added into a fresh flamed and nitrogen purged round-bottomed flask in a glovebox with H_2O and O_2 contents less than 0.1 ppm, and then $\text{Sn}(\text{Oct})_2$ (0.038 g, 0.093 mmol) was added. The mixture was maintained at 80 °C for 48 h. The product was dialyzed (Spectra/Por 4, MWCO 12 000 to 14 000) against Milli-Q water for 1 day to remove unreacted DEGDP. The product was lyophilized and further purified with Sepharose CL-4B in chloroform (CHCl_3) to remove possible unreacted mPEG-PCL. The yield was

58.2%. The control nanogel PEG-polyphosphoester (PEG-DEGDP) nanogel was synthesized according to the literature using DEGDP as the monomer and mPEG as the initiator.⁴⁷

Degradation of TLN by Lipase. Lipase-mediated degradation of TLN was performed at 37 °C in Tris-HCl buffer (0.01 mol L⁻¹, pH 7.4, containing 1 mM MgCl_2 , 50 mM KCl, and 0.1% NaN_3). At the predetermined time, the diameter and count rate of the mixture of TLN with *Pseudomonas* lipase (1 mg mL⁻¹) were measured using dynamic light scattering (DLS) as described in the Supporting Information. The diameter and count rate were also determined after 24 h of incubation with Tris-HCl buffer, phosphate buffered saline (PBS, 0.01 M, pH 7.4), ALP (500 unit mL⁻¹ in Tris-HCl buffer), acetate buffer (0.02 M, pH 5.0), or 10% fetal bovine serum (FBS, Hyclone).

Drug Loading and Release. Vancomycin was loaded into the TLN by mixing TLN (60 mg) with vancomycin (6 mg) at 50 mg mL⁻¹ in DMSO at 60 °C overnight. Water (12 mL) was then added dropwise. The mixture was placed at room temperature for 2 days. Vancomycin was loaded into the PEG-DEGDP nanogel by directly mixing nanogel (30 mg) with vancomycin (3 mg, 10 mg mL⁻¹) in aqueous solution. The vancomycin-loaded TLN (TLN-V) and vancomycin-loaded PEG-DEGDP nanogel were purified by dialysis (Spectra/Por 4, MWCO 12 000 to 14 000) against Milli-Q water for 1 day and ultrafiltrated with Millipore's Amicon Ultra-4 centrifugal filter (NMWL 100 kDa) to remove vancomycin which should keep germ-free throughout. Propidium iodide (PI) was loaded in the same way. To determine the loading efficiency of vancomycin or PI, before the purification, the sample was taken and ultrafiltrated with Millipore's Amicon Ultra-4 centrifugal filter. The concentration of vancomycin or PI in the filtrate was determined by high-performance liquid chromatography (HPLC) or spectrofluorophotometer (RF-5301PC, SHIMADZU Corporation) as described in the Supporting Information. The content of mass loaded into TLN was calculated by subtracting the unloaded amount of vancomycin or PI from the total amount used for drug loading.

The release profiles of vancomycin from the TLN-V under the function of lipase were studied at 37 °C in a medium (Tris-HCl buffer, 0.01 mol L⁻¹, pH 7.4, containing 1 mM MgCl_2 , 50 mM KCl, and 0.1% NaN_3) using a dialysis membrane tubing (Spectra/Por, Float-A-Lyzer, MWCO 12 000 to 14 000). TLN-V (50 μg mL⁻¹ of vancomycin) in the medium without or with *Pseudomonas* lipase (at a final concentration of 0.5 or 1 mg mL⁻¹) or with both *Pseudomonas* lipase (1 mg mL⁻¹) and ALP (500 unit mL⁻¹) was introduced to the dialysis membrane tubing. As a control, the release profiles of vancomycin from vancomycin loaded PEG-DEGDP nanogel were also studied in the Tris-HCl buffer without and with *Pseudomonas* lipase. The tubing was placed in 15 mL of release medium and incubated at 37 °C. At predetermined intervals, all release medium out of the tubing was collected, and the tubing was replaced in 15 mL of fresh medium preincubated at 37 °C. The concentration of vancomycin in the release medium was measured by HPLC analyses.

The stability of TLN-V was studied in the medium of PBS or ALP (500 unit mL⁻¹ in Tris-HCl buffer described above) or acetate buffer (0.02 M, pH 5.0) or 10% FBS. At 24 h, the solution was draw out and ultrafiltrated with Millipore's Amicon Ultra-0.5 centrifugal filter. The filtrate was collected to determine the concentration of vancomycin by HPLC analyses.

The release profiles of vancomycin from the TLN-V under the function of bacteria were studied at 37 °C in a medium with 2 mL of 5% (v/v) TSB in a bacteria cultivation tube. TLN-V (25 μg mL⁻¹ of vancomycin) in the medium without or with bacteria whose optical density at 600 nm (OD_{600}) was 0.1 or 1 was introduced to the tube. Lipase-secreting bacteria (*S. aureus* strain MW2) and low-lipase-secreting bacteria (*Escherichia coli* (*E. coli*) strains Top10 and BL21) were used in this study. At predetermined intervals, 300 μL of the solution was drawn out and ultrafiltrated with Millipore's Amicon Ultra-0.5 centrifugal filter. The filtrate was collected to determine the concentration of vancomycin by HPLC analyses.

Culture of *Staphylococcus aureus* (*S. aureus*) Strains. *S. aureus* strains MW2, NCTC8325, NRS70, NRS71, and NRS72 were grown in

nutrient broth; among them, MW2, NRS70, NRS71, and NRS72 are methicillin-resistant *S. aureus* (MRSA). At the time of cell infection, the OD₆₀₀ of the bacterial suspension was adjusted to 0.5 (corresponding to 2.5×10^8 bacteria). The precise number of bacteria in the suspension was ascertained by plating the diluted bacterial suspension on TSB-Agar A plates (TSA).

Determination of the Inhibitory Effect of TLN-V on *S. aureus* Strains. Vancomycin, TLN-V, or TLN at predetermined concentration in TSB solution (200 μ L) was added into 96-well plates, then 2 μ L of bacterial suspension (*S. aureus* strains MW2, NCTC8325, NRS70, NRS71, and NRS72) whose OD₆₀₀ was 0.5 was added. At 24 or 48 h, the OD₆₀₀ of the bacterial suspension was recorded by BioTek microplates reader.

Cell Culture and Infection with Bacteria. Raw264.7 cells (a gift from Prof. Hai-Ming Wei of School of Life Sciences of University of Science and Technology of China) and HEK293 cells were maintained in tissue culture flasks in DMEM (Dulbecco's Modified Eagle's Medium) containing 10% FBS. For the infection studies, 5×10^4 cells were distributed in 24-well tissue culture plates and were cultured overnight. Cells were infected with 2 μ L of processed bacteria (5×10^5 bacteria). The multiplicity of infection was 10 bacteria per cell. Cells were incubated with the processed bacteria for 1 h to allow for phagocytosis. The wells were then replaced with fresh media containing 1 μ g mL⁻¹ lysostaphin and were incubated for 30 min to eliminate extracellular bacteria. Infected cells were then cultured in fresh media in the presence of vancomycin or TLN-V at the drug dose of 5, 10, or 20 μ g mL⁻¹. Cells exposed to empty TLN or PBS served as controls. Infected cell cultures were terminated after 12 or 24 h. Intracellular viability of *S. aureus* was determined by lysing infected cells with sterile distilled water and plating the lysates on TSA followed by visual inspection for counting of bacterial colonies.

Cellular Uptake of TLN. PI-loaded TLN (TLN-PI, 1 μ L, 10 mg mL⁻¹ in water) or PI was incubated with 100 000 Raw264.7 cells or HEK293 cells in 0.5 mL of complete DMEM culture medium. After incubation at 37 °C for 1, 2, or 4 h, cells were trypsinized, washed with PBS twice, resuspended in 200 μ L of PBS, and subjected to flow cytometric analysis.

For microscopic observation, cells (1×10^5) were seeded on a coverslip in a 24-well tissue culture plate and were cultured overnight. Raw264.7 cells were then infected with 5 μ L of processed *S. aureus* NCTC8325 strains with GFP expression (1×10^6 bacteria). Cells were incubated with the processed bacteria for 1 h to allow for phagocytosis. The wells were then replaced with fresh media containing 1 μ g mL⁻¹ lysostaphin and were incubated for 30 min to eliminate extracellular bacteria. After washing with PBS twice, 5 μ L of TLN-PI were added to distinct wells and incubated at 37 °C for 1 h in 0.5 mL of fresh complete DMEM culture medium. The cells were washed and fixed with 4% formaldehyde, and the slides were mounted and observed with a Zeiss LSM710 Laser Confocal Scanning Microscope imaging system with an upright confocal microscope and a 60 \times objective.

RESULTS AND DISCUSSION

TLN was synthesized by a convenient arm-first procedure^{47–49} as shown in Supporting Information Scheme S1, using an amphiphilic diblock copolymer, namely, monomethoxy poly(ethylene glycol)-*b*-poly(ϵ -caprolactone) (mPEG-PCL), to initiate the ring-opening polymerization of a bifunctional monomer 3-oxapentane-1,5-diyl bis(ethylene phosphate) (DEGDP), similar to our previously reported procedure.⁴⁷ The resulting nanogel particles were contained within the amphiphilic shell of mPEG-PCL which surrounds the cross-linked polyphosphoester core. The chemical structure of the nanogel was confirmed by NMR (Figure 2); the characteristic resonances of methylene protons adjoining phosphoester linkages at 4.17–4.40 ppm were found in the ¹H NMR spectrum. The carbon resonances from the polyphosphoester core were found at 60–70 ppm in the ¹³C NMR spectrum, and

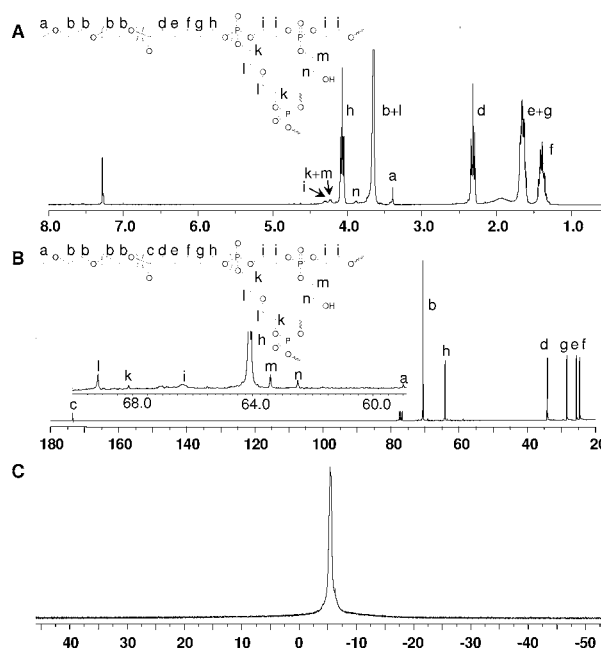


Figure 2. ¹H NMR (A), ¹³C NMR (B), and ³¹P NMR (C) spectra of the TLN in CDCl₃ (ppm).

the ³¹P NMR spectrum also demonstrated the polymerization of the DEGDP monomer via a strong resonance at -5.30 ppm.

Due to the presence of PEG arms, the nanogel can be well-distributed in aqueous and organic solutions including CHCl₃, DMSO, 1,4-dioxane, and tetrahydrofuran (THF). When distributed in THF, the nanogel swelled to an average diameter of 597 ± 49 nm as determined by DLS (Figure 3A), which indicated the successful formation of TLN. The transmission electron microscopy (TEM) image showed that TLN formed a spherical nanoparticle in THF with a core–shell structure lacking the interlayer (Figure 3B). Upon dispersion in water, the hydrophobic PCL segments collapsed and surrounded the polyphosphoester core. The nanoparticles exhibited a diameter around 422 ± 24 nm (Figure 3C). The structure of TLN was further confirmed by TEM (Figure 3D). The nanoparticles took on a spherical morphology and clearly exhibited a triple-layered structure, including a saturated interlayer. The average diameter of the TLN, according to TEM, was around 420 nm, consistent with DLS results, and the average thickness of the interlayer was approximately 29 nm. It should be mentioned that the micelles formed by the mPEG-PCL macroinitiator alone in water exhibited an average diameter of 56 nm (Figure 3E), much smaller than that of TLN. The micelles vanished in THF; this serves as a demonstration for the successful formation of TLN. The ¹H NMR spectrum of the TLN in D₂O (Figure 3F) showed that signals assigned to protons of the PCL block diminished and broadened, which also indicated the collapse of hydrophobic PCL layer.⁵⁰

Pseudomonas lipase is known to degrade PCL.⁵¹ We then analyzed the size and count rate of the TLN in culture medium either in the absence or presence of *Pseudomonas* lipase to demonstrate the enzymatic degradation of TLN. As shown in Figure 4, culturing the TLN for 24 h in Tris-HCl buffer without the enzyme did not significantly change the diameter and count rate. However, with *Pseudomonas* lipase, PCL degradation led to rapid aggregation of nanoparticles, resulting in an increased average diameter of 910 ± 270 nm at 1 h which further

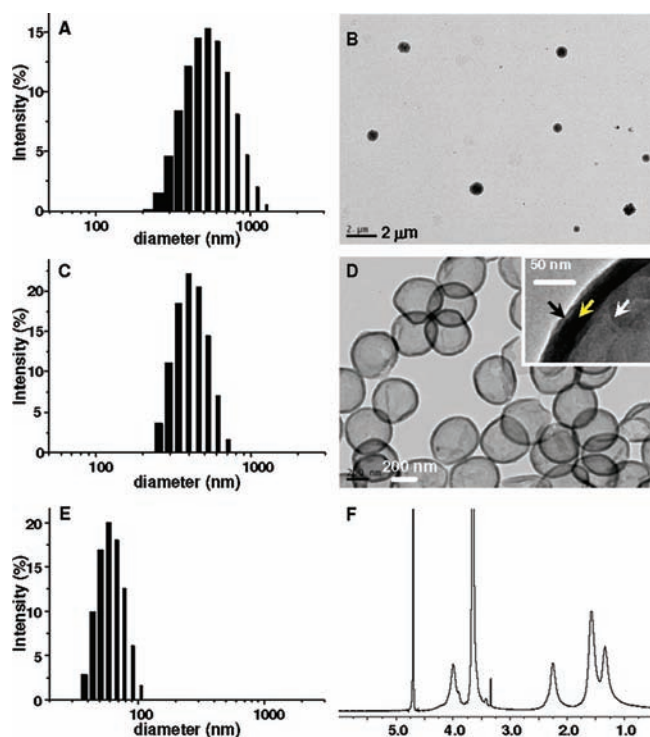


Figure 3. (A and B) The size distribution (A) and TEM image (B) of the TLN in THF. The scale bar represents 1 μm ; (C and D) the size distribution (C) and TEM image (D) of TLN in water. The white arrow in the insert picture of (D) indicates the cross-linked polyphosphoester core; the yellow arrow indicates the PCL molecular fence, and the black arrow indicates the shell of PEG. The scale bar represents 200 nm; (E) the size distribution of the micelles of mPEG-PCL; (F) ^1H NMR spectrum of the TLN in D_2O (ppm).

increased to 1120 ± 290 at 2 h. The diameter as measured by DLS subsequently decreased with the extended culture time as precipitation was observed (Figure S3, Supporting Information). Accordingly, the count rates continuously decreased with increased culture time in the presence of the enzyme. This parameter represents the light scattering intensity of the sample which displays the number of photons detected per second (displayed in kcps-kilo counts per second). Therefore it can be used for comparison in the scattering intensity between samples and indicates the particle concentration in the solution. It can be concluded that the degradation of PCL by *Pseudomonas* lipase resulted in the detachment of the PEG layer and aggregation. It was also demonstrated that the TLN was stable in buffer at various pHs (e.g., PBS, pH 7.4, or acetate buffer, pH 5.0). On the other hand, ALP did not significantly affect the stability of TLN in the absence of *Pseudomonas* lipase. Moreover, although count rate increased when TLN was incubated in 10% FBS, the diameter of TLN was not dramatically affected after 24 h of incubation, indicative of the stability of TLN in serum-containing conditions. It should be mentioned that particles could be detected in FBS solution by DLS, likely due to light scattering phenomenon of FBS itself, which contributed to the higher count rate for TLN in FBS.

We then examined whether the TLN could act as a carrier for on-demand drug delivery to treat bacterial infections. It was hypothesized that the compact PCL molecular fence would inhibit undesired antibiotic leakage but in the presence of lipase or lipase-secreting bacteria would degrade and release the antibiotic to kill the bacteria. Our previous study demonstrated

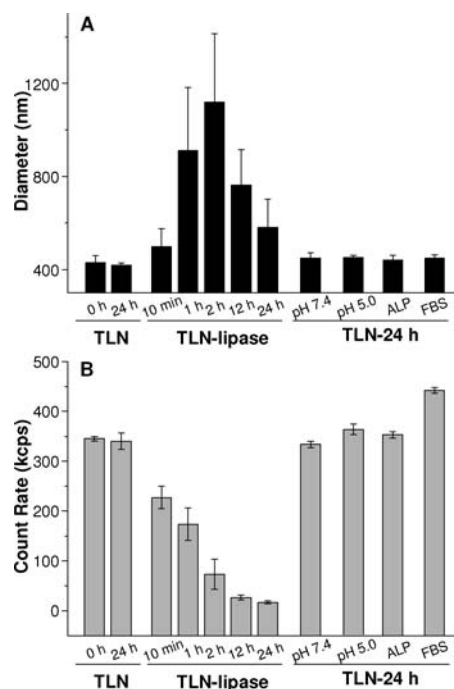


Figure 4. The diameter (A, intensity statistics) and count rate (B) of the TLN after culturing in medium for different time periods. TLN and TLN-lipase represent that the TLN was cultured in Tris-HCl buffer (0.01 M, pH 7.4) without or with 1 mg mL^{-1} *Pseudomonas* lipase, respectively. TLN-24 h represents that the TLN was cultured for 24 h in PBS (0.01 M, pH 7.4), acetate buffer (0.02 M, pH 5.0), ALP (500 unit mL^{-1} in Tris-HCl buffer, pH 7.4), or 10% fetal bovine serum (FBS).

that the PEG-armed polyphosphoester core cross-linked nanogel could potentially deliver the hydrophilic drug doxorubicin.⁴⁷ In this study, we encapsulated the antibiotic vancomycin into the cross-linked polyphosphoester core and attempted to demonstrate the “on-demand” drug release and antibacterial activity against *S. aureus*, the leading cause of nosocomial infections as the model bacterium.⁵² To encapsulate the drug, vancomycin and the TLN were dissolved in DMSO, and the mixture was slightly shaken overnight at 60 °C. Afterward, water was dripped into the solution and the PCL interlayer collapsed to besiege the polyphosphoester core. The organic solvent and any unencapsulated drug were removed by dialysis in water and ultrafiltrated to obtain vancomycin-loaded TLN (TLN-V). The loading weight ratio of drug to TLN was $4.2 \pm 0.3\%$, and the drug loading efficiency was $42.4 \pm 0.03\%$ when the feed weight ratio of vancomycin to TLN was 1:10. After loaded with vancomycin, the particle size and surface property of TLN did not change significantly; diameter was 429 ± 31 nm and zeta potential was -20.6 ± 0.8 mV.

The release behavior of vancomycin from the TLN-V was monitored in Tris-HCl buffer at pH 7.4 either with or without the presence of *Pseudomonas* lipase. Not surprisingly, the release of vancomycin from the TLN-V was minimal in the buffer without lipase: $10 \pm 1\%$ cumulative release of total encapsulated drug over 48 h of incubation (Figure 5A). However, when the TLN-V was incubated with *Pseudomonas* lipase, rapid release of vancomycin was observed due to the rapid degradation of the PCL interlayer. The release rate of vancomycin was dependent on the concentration of lipase, since more vancomycin was released with higher lipase

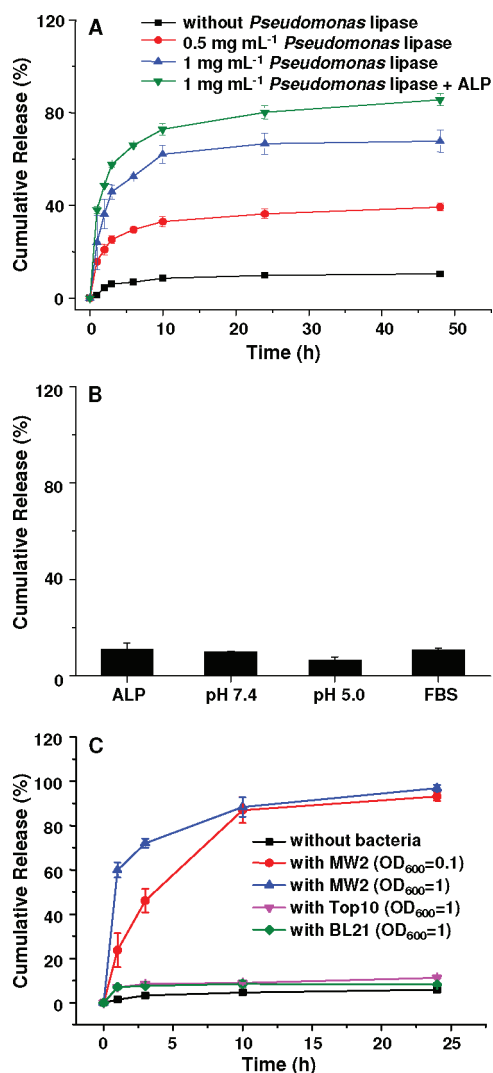


Figure 5. (A) Cumulative release of vancomycin from vancomycin-loaded TLN (TLN-V). TLN-V was cultured in Tris-HCl buffer (0.01M, pH7.4) in the absence or presence of enzyme(s). The concentration of ALP was 500 unit mL⁻¹. (B) Cumulative release of vancomycin from TLN-V after 24 h culture in Tris-HCl buffer containing 500 unit mL⁻¹ ALP, PBS at pH 7.4, acetate buffer at pH 5.0, or 10% FBS. (C) Cumulative release of vancomycin from TLN-V in the absence or presence of *S. aureus* MW2 at an OD₆₀₀ value of 0.1 or 1.0 or the presence of *E. coli* strains Top10 and BL21 at an OD₆₀₀ value of 1.0.

concentrations. Furthermore, culturing the TLN-V in medium with both *Pseudomonas* lipase and ALP led to an even faster release of and increased total release amount of vancomycin. The cumulative release of total encapsulated drug over 48 h reached 86 ± 3%. The degradation of the PCL fence by *Pseudomonas* lipase facilitated the degradation of the polyphosphoester core by ALP. The cleavage points of enzymes and the reaction scheme are shown in Supporting Information Scheme S2. Thus the release rate and amount were increased. However, ALP alone could not accelerate the release of vancomycin from TLN-V even in 24 h, as shown in Figure 5B, indicating that the PCL molecular fence separated the polyphosphoester core from ALP. As indicated in Figure 5B, only minimal release of drug was observed in 24 h when TLN-V was incubated with PBS or acetate buffer at pH 5.0 or 10% FBS.

To prove that the triple-layered construct is indeed necessary to achieve the desired effect, amphiphilic block polymer mPEG-PCL and PEG-polyphosphoester nanogel (PEG-DEGDP) were conducted as controls. To test whether the hydrophilic vancomycin can be loaded by the hydrophobic PCL domain, we employed the same loading procedure to load vancomycin. The DLC was lower than 0.1%, indicating that the hydrophilic vancomycin cannot be loaded within the PCL domain. In another control experiment, PEG-DEGDP nanogel without a PCL interlayer was prepared and used to load vancomycin with a DLC that was 8.5%, comparable to that of the triple-layered nanogel. Moreover, the release behavior of vancomycin from the loaded PEG-DEGDP nanogel exhibited a burst release with or without *Pseudomonas* lipase (Figure S4, Supporting Information), which was similar to the release behavior of vancomycin from TLN-V under catalysis of lipase (Figure 5A). The above results combined demonstrated that the drug resided in the polyphosphoester core but not in the PCL interlayer, and the PCL interlayer was necessary to achieve the desired effect.

To further demonstrate that the release of vancomycin from the TLN-V can be triggered by bacteria, we incubated TLN-V with MW2, a methicillin-resistant strain of *S. aureus*, which showed secretory lipase activity as demonstrated by the tributyrin agar test (Figure S5A, Supporting Information) and determined the release profile of vancomycin. As shown in Figure 5C, only 1 ± 0.4% and 6 ± 1% of total encapsulated vancomycin was released from the TLN-V when they were incubated with 5% Bacto Tryptic Soy Broth (TSB) for 1 and 24 h, respectively. On the contrary, when incubated with the MW2 strain in 5% TSB, the TLN-V released vancomycin very quickly. The cumulative release of vancomycin reached 24 ± 8% of total encapsulated drug in 1 h when the TLN-V was incubated with the MW2 strain at an optical density at 600 nm (OD₆₀₀) of 0.1. Drug release was further accelerated with a higher concentration of bacteria, and 60 ± 3% of the payloads were released in 1 h when incubated with the MW2 strain at an OD₆₀₀ value of 1.0. In both cases, more than 80% of total encapsulated drug was released from the TLN-V within 10 h, and nearly the entire payloads were released when incubated for 24 h. In the system with bacteria, active enzymes like lipase, phosphatases, and phospholipase were secreted,⁵³ which degrade the PCL molecular fence and polyphosphoester core resulting in the release of the drug molecules. To prove that TLN was destructed by lipase, two *E. coli* strains Top10 and BL21 with low lipase secretions (Supporting Information Figure S5B) were used as controls. After incubation of TLN-V with Top10 and BL21, the release of vancomycin was only slightly higher than that without bacteria but significantly lower than that of incubation with lipase-secreting bacteria (Top10: 11 ± 0.1%, BL21: 8 ± 0.7% vs MW2: more than 90% after 24 h of incubation) (Figure 5C). These results demonstrated that lipase-secreting bacteria could trigger the rapid release of vancomycin from the TLN-V.

After having demonstrated that bacterial lipase triggered drug release from the TLN-V, we further examined the ability of TLN-V to inhibit the growth of *S. aureus* strains; NCTC8325, MW2, NRS70, NRS71, and NRS72, all of which exhibited secreted lipase (Figure S5A, Supporting Information). TLN-V was incubated with bacteria at different doses of vancomycin in 5% TSB, followed by OD₆₀₀ measurements to evaluate bacterial growth. As shown in Figure 6, after 48 h of incubation, TLN-V better inhibited the growth of *S. aureus* strains than vancomycin

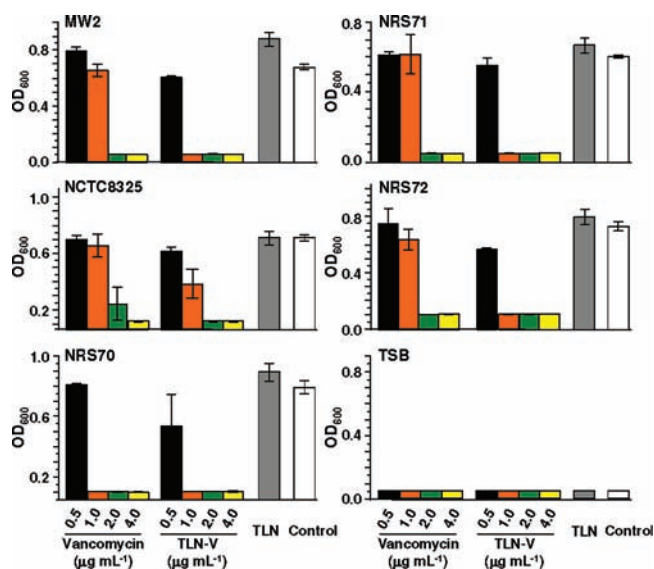


Figure 6. Dose-dependent growth inhibition of *S. aureus* strains at 48 h in the presence of free vancomycin, TLN-V, or TLN ($95.2 \mu\text{g mL}^{-1}$, equal to the concentration of TLN in culture that the bacteria were treated with TLN-V at a vancomycin concentration of $4 \mu\text{g mL}^{-1}$). The concentration given in TLN-V represents the concentration of vancomycin loaded in TLN-V. The data are expressed as mean \pm standard deviation of three replicates. Standard deviation is indicated by the error bars. The control is bacteria in Bacto Tryptic Soy Broth (TSB).

alone at the same dosage concentration, although TLN alone stimulated a slight elevation in the growth of bacteria at high concentrations for unclear reasons. Similar results were observed when the bacteria were incubated with TLN-V for 24 h (Figure S6, Supporting Information). This superior inhibition may have been due to better interactions between TLN-V and bacteria compared to free vancomycin. This demonstrated that TLN-V had the ability to inhibit the growth of the *S. aureus* strains, suggesting that the vancomycin was released on-demand from the nanoparticles by *S. aureus* strains. It should be pointed out that when vancomycin, TLN-V, or TLN alone were incubated with TSB, no bacteria were detected, demonstrating that no bacterial contamination occurred during the experiment.

We next examined if TLN-V could deliver vancomycin into bacterial-infected cells since vancomycin itself and many other antibiotics exhibit poor intracellular penetration into cells, restricting their application against cellular infections caused by *S. aureus*.^{54–57} Considering that *S. aureus* can survive within macrophages, protecting them against the bactericidal action of antibiotics,^{37,58} and that intraphagocytic survival *S. aureus* causes recurring infections,³⁸ we then performed experiments on macrophages to determine the inhibitory effect of TLN-V on bacterial growth in cells. To first demonstrate that TLN can penetrate the cell membrane, we used a cell membrane impermeable fluorescent dye, propidium iodide (PI), as the model. PI was encapsulated into TLN to form TLN-PI, and the loading weight ratio of PI to TLN was 4.6%, corresponding to a loading efficiency of 46%. The diameter of TLN-PI was 412 ± 9 nm, and the zeta potential was -20.1 ± 0.6 mV, similar to those of TLN-V. The resulting TLN-PI was further incubated with Raw264.7 cells, a mouse macrophage cell line. Flow cytometric analyses after different incubation periods revealed that the fluorescence intensities of PI in Raw264.7 cells were

enhanced with prolonged incubation (Figure 7A), while in parallel experiments free PI treatment showed much lower

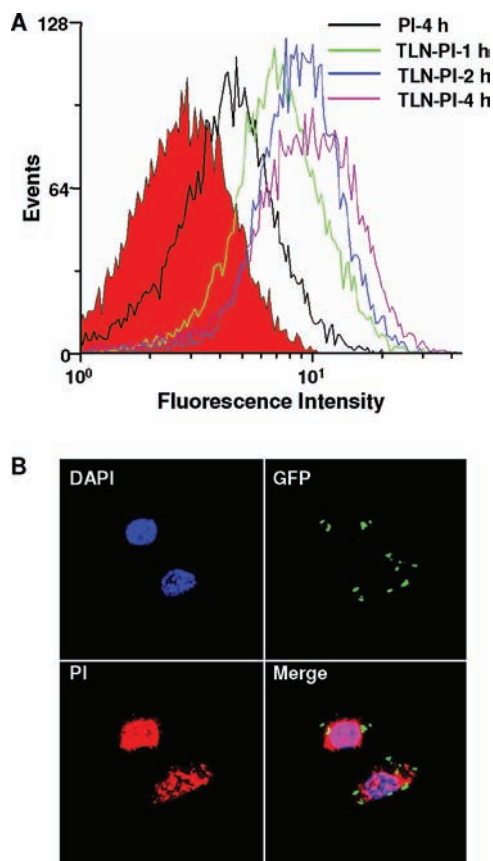


Figure 7. Cellular uptake of propidium iodide (PI)-loaded TLN (TLN-PI) over time as analyzed by flow cytometric analyses (A), and the internalization of TLN-PI by Raw264.7 cells infected with the GFP-expressing strain NCTC8325 (B).

cellular fluorescence intensity. Cellular uptake and release of PI from TLN-PI in the Raw264.7 cells with or without *S. aureus* strain NCTC8325 infection were analyzed by flow cytometric analyses. Cellular fluorescence of infected cells after incubation with TLN-PI was stronger than that of healthy cells after the same treatment (Figure S7, Supporting Information); while in the control experiment, no fluorescence enhancement was observed. The results suggest that the burst release of loaded drug could only be triggered in the infected cells. On the other hand, to further illustrate the entry of TLN-PI into cells, we infected Raw264.7 cells with green fluorescent protein (GFP)-expressing *S. aureus* NCTC8325 strain. Afterward, we incubated the bacteria-infected cells with TLN-PI. Observation using confocal laser scanning microscopy (CLSM) showed that PI and the NCTC8325 strain colocalized in cells (Figure 7B), indicating that TLN could enhance PI entry into bacteria-infected cells. It is notable that fluorescent PI was seen in the nuclei, suggesting that PI was released from TLN in the bacteria-infected macrophages. The enhanced cellular uptake of PI delivered by TLN into HEK293 cells was also demonstrated by FACS and CLSM (Figure S8, Supporting Information).

The ability of TLN-V to kill intracellular bacteria was then examined by counting the colony forming units (CFU) of surviving intracellular bacteria after incubating TLN-V with Raw264.7 cells infected with the MW2 strain. TLN-V showed a

concentration and time dependent function of intracellular bacterial growth inhibition. As shown in Figure 8, after 12 or 24

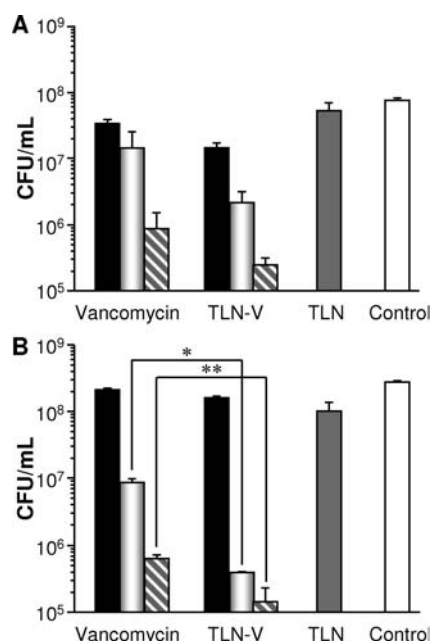


Figure 8. Intracellular survival of *S. aureus* MW2 in Raw264.7 cells. Infected cells were cultured with vancomycin, TLN-V, or empty TLN ($476.2 \mu\text{g mL}^{-1}$, equal to the concentration of TLN in culture that the cells were treated with TLN-V at a vancomycin concentration of $20 \mu\text{g mL}^{-1}$) or left untreated (control). The final concentration of vancomycin in the culture was 5 (solid bar), 10 (gray bar), or 20 (striped bar) $\mu\text{g mL}^{-1}$ when it was applied. The incubation was terminated after 12 h (a) or 24 h (b) to determine the intracellular survival of *S. aureus*. CFU, colony-forming units. * represents $p < 0.05$ and ** represents $p < 0.01$ determined by Student's *t* test.

h of incubation, TLN-V exhibited significantly better inhibitory capability against intracellular bacteria compared to free vancomycin, particularly at higher doses. TLN alone had no inhibitory effect, showing similar CFU as the control that received no treatment. Vancomycin or TLN-V treatment of MW2-infected Raw264.7 cells showed little inhibition of intracellular bacterial growth at a dose of $5 \mu\text{g mL}^{-1}$. When the absolute concentration of vancomycin was increased to $10 \mu\text{g mL}^{-1}$, the CFU of surviving intracellular bacteria, treated by TLN-V, were about 7 and 22 times lower than that in cells treated with free vancomycin at 12 and 24 h, respectively. At a dose of $20 \mu\text{g mL}^{-1}$, TLN-V showed 3- and 4-fold better inhibitory capability at 12 and 24 h, respectively. This revealed the superior inhibition of intracellular bacterial growth by TLN-V, which can be accounted for by efficient vancomycin delivery by TLN-V into the bacteria-infected Raw264.7 cells. TLN-V also exhibited better inhibitory capacity compared to free vancomycin in four other intracellular *S. aureus* strains (Figure S9, Supporting Information). To further prove that the TLN-V releases its drug content in the infected mammalian cells, HEK293 cells were infected with MW2 and treated with TLN-V to assess the inhibitory effect. As shown in Supporting Information Figure S10, TLN-V exhibited significantly better inhibition of intracellular bacteria when compared with the free vancomycin treatment. These results demonstrate that TLN-V can deliver vancomycin into the bacteria-infected cells, release their cargo, and kill intracellular pathogens very efficiently. It is

worth noting that vancomycin, TLN, or TLN-V had no effect on the viabilities of Raw264.7 cells and HEK293 cells (Figure S11, Supporting Information).

CONCLUSIONS

In conclusion, a novel nanoparticulate platform for on-demand delivery of antibiotics, in which bacterial lipases were utilized to trigger the release of antibiotics by degrading the hydrophobic poly(ϵ -caprolactone) interlayer of a polymeric triple-layered nanogel, was developed. The triple-layered nanogel was synthesized by a convenient “arm-first” procedure and insertion of the lipase-sensitive PCL interlayer endowed the drug-loaded nanogel with an “on-demand” release feature, exhibiting little drug release in the absence of lipase or lipase-secreting bacteria. However, rapid drug release was observed in the presence of lipase or lipase-secreting bacteria. We demonstrated that extracellular bacterial growth was effectively inhibited by the antibiotics released by the nanogel. Furthermore, the nanogel transported the drug into bacteria-infected cells and efficiently released the drug to kill intracellular bacteria. Considering the tremendous abundance of lipase during bacterial infection and although vancomycin was used as the model antibiotic in this study, this technique can be broadly applied to deliver a variety of other antibiotics for the treatment of extracellular and intracellular bacterial infections.

ASSOCIATED CONTENT

Supporting Information

Synthesis of DEGDP and mPEG-PCL, characterizations, synthesis scheme of TLN, bacterial lipase test of *S. aureus*, dose-dependent growth inhibition of *S. aureus* strains at 24 h, intracellular survival of other four *S. aureus* in Raw264.7 cells, MTT assay against Raw264.7, complete ref 2. This material is available free of charge via the Internet at <http://pubs.acs.org>.

AUTHOR INFORMATION

Corresponding Author

jwang699@ustc.edu.cn, sunb@ustc.edu.cn

Author Contributions

‡These authors contributed equally.

Author Contributions

The manuscript was written through contributions of all authors. All authors have given approval to the final version of the manuscript.

Notes

The authors declare no competing financial interest.

ACKNOWLEDGMENTS

This work was supported by the National Basic Research Program of China (973 Programs, 2010CB934001, 2009CB930301), the National Natural Science Foundation of China (51125012, 20974105, 50733003), the Fundamental Research Funds for the Central Universities (WK2070000008), and the Ministry of Education of China (SRFDP Contract 20113402130008).

REFERENCES

- LaVan, D. A.; McGuire, T.; Langer, R. *Nat. Biotechnol.* **2003**, *21*, 1184–1191.
- Ashley, C. E.; et al. *Nat. Mater.* **2011**, *10*, 476–476.
- Gullotti, E.; Yeo, Y. *Mol. Pharmaceutics* **2009**, *6*, 1041–1051.

- (4) Slowing, I. I.; Vivero-Escoto, J. L.; Wu, C. W.; Lin, V. S. Y. *Adv. Drug Delivery Rev.* **2008**, *60*, 1278–1288.
- (5) Meng, H. A.; Xue, M.; Xia, T. A.; Zhao, Y. L.; Tamanoi, F.; Stoddart, J. F.; Zink, J. I.; Nel, A. E. *J. Am. Chem. Soc.* **2010**, *132*, 12690–12697.
- (6) Muhammad, F.; Guo, M. Y.; Qi, W. X.; Sun, F. X.; Wang, A. F.; Guo, Y. J.; Zhu, G. S. *J. Am. Chem. Soc.* **2011**, *133*, 8778–8781.
- (7) Liu, R.; Zhang, Y.; Zhao, X.; Agarwal, A.; Mueller, L. J.; Feng, P. Y. *J. Am. Chem. Soc.* **2010**, *132*, 1500–1501.
- (8) Zhu, Y. F.; Shi, J. L.; Shen, W. H.; Dong, X. P.; Feng, J. W.; Ruan, M. L.; Li, Y. S. *Angew. Chem., Int. Ed.* **2005**, *44*, 5083–5087.
- (9) Lai, C. Y.; Trewyn, B. G.; Jeftinija, D. M.; Jeftinija, K.; Xu, S.; Jeftinija, S.; Lin, V. S. Y. *J. Am. Chem. Soc.* **2003**, *125*, 4451–4459.
- (10) Sauer, A. M.; Schlossbauer, A.; Ruthardt, N.; Cauda, V.; Bein, T.; Brauchle, C. *Nano Lett.* **2010**, *10*, 3684–3691.
- (11) Kim, H.; Kim, S.; Park, C.; Lee, H.; Park, H. J.; Kim, C. *Adv. Mater.* **2010**, *22*, 4280–4283.
- (12) Luo, Z.; Cai, K. Y.; Hu, Y.; Zhao, L.; Liu, P.; Duan, L.; Yang, W. H. *Angew. Chem., Int. Ed.* **2011**, *50*, 640–643.
- (13) Schlossbauer, A.; Warncke, S.; Gramlich, P. M. E.; Kecht, J.; Manetto, A.; Carell, T.; Bein, T. *Angew. Chem., Int. Ed.* **2010**, *49*, 4734–4737.
- (14) Chen, C. E.; Geng, J.; Pu, F.; Yang, X. J.; Ren, J. S.; Qu, X. G. *Angew. Chem., Int. Ed.* **2011**, *50*, 882–886.
- (15) Bernardos, A.; Mondragón, L.; Aznar, E.; Marcos, M. D.; Martínez-Máñez, R.; Sancenón, F.; Soto, J.; Barat, J. M.; Pérez-Payá, E.; Guillem, C.; Amorós, P. *ACS Nano* **2010**, *4*, 6353–6368.
- (16) Park, C.; Kim, H.; Kim, S.; Kim, C. *J. Am. Chem. Soc.* **2009**, *131*, 16614–16615.
- (17) Thornton, P. D.; Heise, A. *J. Am. Chem. Soc.* **2010**, *132*, 2024–2028.
- (18) Patel, K.; Angelos, S.; Dichtel, W. R.; Coskun, A.; Yang, Y. W.; Zink, J. I.; Stoddart, J. F. *J. Am. Chem. Soc.* **2008**, *130*, 2382–2383.
- (19) Climent, E.; Bernardos, A.; Martínez-Máñez, R.; Maquieira, A.; Marcos, M. D.; Pastor-Navarro, N.; Puchades, R.; Sancenón, F.; Soto, J.; Amorós, P. *J. Am. Chem. Soc.* **2009**, *131*, 14075–14080.
- (20) Zhao, Y. N.; Trewyn, B. G.; Slowing, I. I.; Lin, V. S. Y. *J. Am. Chem. Soc.* **2009**, *131*, 8398–8400.
- (21) Zhu, C. L.; Lu, C. H.; Song, X. Y.; Yang, H. H.; Wang, X. R. *J. Am. Chem. Soc.* **2011**, *133*, 1278–1281.
- (22) Thomas, C. R.; Ferris, D. P.; Lee, J. H.; Choi, E.; Cho, M. H.; Kim, E. S.; Stoddart, J. F.; Shin, J. S.; Cheon, J.; Zink, J. I. *J. Am. Chem. Soc.* **2010**, *132*, 10623–10625.
- (23) Kong, S. D.; Zhang, W. Z.; Lee, J. H.; Brammer, K.; Lal, R.; Karin, M.; Jin, S. H. *Nano Lett.* **2010**, *10*, 5088–5092.
- (24) Ruiz-Hernández, E.; Baeza, A.; Vallet-Regí, M. *ACS Nano* **2011**, *5*, 1259–1266.
- (25) Lin, Q. N.; Huang, Q.; Li, C. Y.; Bao, C. Y.; Liu, Z. Z.; Li, F. Y.; Zhu, L. Y. *J. Am. Chem. Soc.* **2010**, *132*, 10645–10647.
- (26) Ferris, D. P.; Zhao, Y. L.; Khashab, N. M.; Khatib, H. A.; Stoddart, J. F.; Zink, J. I. *J. Am. Chem. Soc.* **2009**, *131*, 1686–1688.
- (27) Vivero-Escoto, J. L.; Slowing, I. I.; Wu, C. W.; Lin, V. S. Y. *J. Am. Chem. Soc.* **2009**, *131*, 3462–3463.
- (28) Liu, N. G.; Dunphy, D. R.; Atanassov, P.; Bunge, S. D.; Chen, Z.; Lopez, G. P.; Boyle, T. J.; Brinker, C. J. *Nano Lett.* **2004**, *4*, 551–554.
- (29) Cheng, K.; Peng, S.; Xu, C. J.; Sun, S. H. *J. Am. Chem. Soc.* **2009**, *131*, 10637–10644.
- (30) Katagiri, K.; Imai, Y.; Koumoto, K.; Kaiden, T.; Kono, K.; Aoshima, S. *Small* **2011**, *7*, 1683–1689.
- (31) Dai, J.; Cheng, D.; Zou, S. Y.; Shuai, X. T. *Angew. Chem., Int. Ed.* **2011**, *50*, 9404–9408.
- (32) Pornpattananakul, D. P.; Zhang, L.; Olson, S.; Aryal, S.; Obonyo, M.; Vecchio, K.; Huang, C. M.; Zhang, L. F. *J. Am. Chem. Soc.* **2011**, *133*, 4132–4139.
- (33) Tang, S. H.; Huang, X. Q.; Chen, X. L.; Zheng, N. F. *Adv. Funct. Mater.* **2010**, *20*, 2442–2447.
- (34) Ning, X. H.; Lee, S.; Wang, Z. R.; Kim, D.; Stubblefield, B.; Gilbert, E.; Murthy, N. *Nat. Mater.* **2011**, *10*, 602–607.
- (35) Viswanathan, V. K.; Hodges, K.; Hecht, G. *Nat. Rev. Microbiol.* **2009**, *7*, 1–10.
- (36) Alekshun, M. N.; Levy, S. B. *Cell* **2007**, *128*, 1037–1050.
- (37) Foster, T. J. *Nat. Rev. Microbiol.* **2005**, *3*, 948–958.
- (38) Proctor, R. A.; von Eiff, C.; Kahl, B. C.; Becker, K.; McNamara, P.; Herrmann, M.; Peters, G. *Nat. Rev. Microbiol.* **2006**, *4*, 295–305.
- (39) Nederberg, F.; Zhang, Y.; Tan, J. P. K.; Xu, K. J.; Wang, H. Y.; Yang, C.; Gao, S. J.; Guo, X. D.; Fukushima, K.; Li, L. J.; Hedrick, J. L.; Yang, Y. Y. *Nat. Chem.* **2011**, *3*, 409–414.
- (40) Zhao, Y. Y.; Tian, Y.; Cui, Y.; Liu, W. W.; Ma, W. S.; Jiang, X. Y. *J. Am. Chem. Soc.* **2010**, *132*, 12349–12356.
- (41) Hancock, R. E. W.; Sahl, H. G. *Nat. Biotechnol.* **2006**, *24*, 1551–1557.
- (42) Briones, E.; Colino, C. I.; Lanao, J. M. *J. Controlled Release* **2008**, *125*, 210–227.
- (43) Drulis-Kawa, Z.; Dorotkiewicz-Jach, A. *Int. J. Pharm.* **2010**, *387*, 187–198.
- (44) Arpigny, J. L.; Jaeger, K. E. *Biochem. J.* **1999**, *343*, 177–183.
- (45) Jaeger, K. E.; Ransac, S.; Dijkstra, B. W.; Colson, C.; Vanheuver, M.; Misset, O. *FEMS Microbiol. Rev.* **1994**, *15*, 29–63.
- (46) Kricheldorf, H. R.; Kreiser-Saunders, I.; Stricker, A. *Macromolecules* **2000**, *33*, 702–709.
- (47) Xiong, M. H.; Wu, J.; Wang, Y. C.; Li, L. S.; Liu, X. B.; Zhang, G. Z.; Yan, L. F.; Wang, J. *Macromolecules* **2009**, *42*, 893–896.
- (48) Li, W. W.; Matyjaszewski, K. *J. Am. Chem. Soc.* **2009**, *131*, 10378–10379.
- (49) Goh, T. K.; Tan, J. F.; Guntari, S. N.; Satoh, K.; Blencowe, A.; Kamigaito, M.; Qiao, G. G. *Angew. Chem., Int. Ed.* **2009**, *48*, 8707–8711.
- (50) Wang, Y. C.; Tang, L. Y.; Sun, T. M.; Li, C. H.; Xiong, M. H.; Wang, J. *Biomacromolecules* **2008**, *9*, 388–395.
- (51) Chawla, J. S.; Amiji, M. M. *Int. J. Pharm.* **2002**, *249*, 127–138.
- (52) Lowy, F. D. *N. Engl. J. Med.* **1998**, *339*, 520–532.
- (53) Schmiel, D. H.; Miller, V. L. *Microbes Infect.* **1999**, *1*, 1103–1112.
- (54) Onyeji, C. O.; Nightingale, C. H.; Marangos, M. N. *Infection* **1994**, *22*, 338–342.
- (55) Pumerantz, A.; Muppidi, K.; Agnihotri, S.; Guerra, C.; Venketaraman, V.; Wang, J.; Betageri, G. *Int. J. Antimicrob. Agents* **2011**, *37*, 140–144.
- (56) Vanderawera, P.; Matsumoto, T.; Husson, M. *J. Antimicrob. Chemother.* **1988**, *22*, 185–192.
- (57) Bakkerwoudenberg, I. A. J. M. *Adv. Drug Delivery Rev.* **1995**, *17*, 5–20.
- (58) Garzoni, C.; Kelley, W. L. *Trends Microbiol.* **2009**, *17*, 59–65.